2-13-2009

Basal mechanics of ice streams: Insights from the stick-slip motion of Whillans Ice Stream, West Antarctica

J. Paul Winberry

Sridhar Anandakrishnan

Richard B. Alley

Robert A. Bindschadler

Matt A. King

Basal mechanics of ice streams: Insights from the stick-slip motion of Whillans Ice Stream, West Antarctica

J. Paul Winberry,[1,2] Sridhar Anandakrishnan,[2] Richard B. Alley,[2] Robert A. Bindschadler,[3] and Matt A. King[4]

Received 16 April 2008; revised 23 October 2008; accepted 15 November 2008; published 13 February 2009.

[1] The downstream portion of Whillans Ice Stream, West Antarctica, moves primarily by stick-slip motion. The observation of stick-slip motion suggests that the bed is governed by velocity-weakening physics and that the basal physics is more unstable than suggested by laboratory studies. The stick-slip cycle of Whillans Ice Plain exhibits substantial variability in both the duration of sticky periods and in slip magnitude. To understand this variability, we modeled the forces acting on the ice stream during the stick phase of the stick-slip cycle. The ocean tides introduce changes in the rate at which stress is applied to the ice plain. Increased loading rates promote earlier failure and vice versa. Results show that the bed of Whillans Ice Stream strengthens over time (healing) during the quiescent intervals in the stick-slip cycle, with the bed weakening during slip events. The time-dependent strengthening of the ice plain bed following termination of slip events indicates that the strength of the bed may vary by up to 0.35 kPa during the course of a single day.

Citation: Winberry, J. P., S. Anandakrishnan, R. B. Alley, R. A. Bindschadler, and M. A. King (2009), Basal mechanics of ice streams: Insights from the stick-slip motion of Whillans Ice Stream, West Antarctica, *J. Geophys. Res.*, *114*, F01016, doi:10.1029/2008JF001035.

1. Introduction

[2] The fast-flowing ice streams that drain ice sheet interiors have received much attention in recent decades because they provide the main avenue for the transport of large volumes of ice to the world's oceans [*Joughin and Tulaczyk*, 2002]. Seismic studies in the mid-1980s [*Rooney et al.*, 1987; *Blankenship et al.*, 1986], followed later by direct borehole observations [*Engelhardt et al.*, 1990], revealed that rapid motion of some ice streams is enabled by efficient basal lubrication by a spatially pervasive weak subglacial till and high subglacial water pressures. Determining the appropriate physics for basal motion of ice streams is fundamental to the development of an ice stream model for predicting the behavior of large ice sheets. However, divergent rheologic models have been proposed to relate applied basal shear stress to basal motion, ranging from linear-viscous [*Alley et al.*, 1987] to rate-independent plastic models [*Tulaczyk et al.*, 2000a], with the possibility that both apply depending on strain history [*Rathbun et al.*, 2008]. Critical to validation and selection of the appropriate model are field-based observations that document how ice stream motion responds to variable forcing. However, in situ constraints on large ice streams remain limited [*Engelhardt and Kamb*, 1998]. Recent observations have revealed that the ocean tides introduce large daily to yearly fluctuations in ice stream velocities [*Anandakrishnan et al.*, 2003; *Bindschadler et al.*, 2003b; *Gudmundsson*, 2007; *Murray et al.*, 2007], providing a potential in situ mechanism for deciphering the appropriate basal physics for ice streams. Successful modeling of measured tidal forcings and the subsequent ice stream response should provide field-based insight into the basal flow mechanism of ice streams.

[3] Perhaps the most spectacular example of tidally-influenced ice stream flow is the lurching behavior observed in the lower reaches of Whillans Ice Stream (WIS)(formerly known as Ice Stream B). The downstream 150 km portion of WIS consists of a wide (>100 km) region of lightly grounded ice [*Bindschadler*, 1993], referred to as the Whillans Ice Plain (WIP). Although the average annual velocity of the WIP exceeds 300 m/a, typical of other ice streams, most of this motion is accommodated in short bursts (<1 h) that are separated by long (6–25 hours) stagnant periods [*Bindschadler et al.*, 2003b]. The unsteady motion observed on WIP bears a striking resemblance to stick-slip motion observed during earthquakes [e.g, *Brace and Byerlee*, 1966].

[4] In this manuscript, we explore the underlying physics responsible for ice stream stick-slip motion, and its application to ice stream mechanics. We first introduce the fundamental mechanics of stick-slip motion, allowing first-order insight into ice stream basal rheology. The characteristics of the WIP stick-slip cycle are then reviewed using a recently

[1]Department Geological Sciences, Central Washington University, Ellensburg, Washington, USA.
[2]Center for Remote Sensing of Ice Sheets, Department of Geosciences, Penn State University, University Park, Pennsylvania, USA.
[3]Hydrospheric and Biospheric Sciences Laboratory, NASA Goddard Space Flight Center, Greenbelt, Maryland, USA.
[4]School of Civil Engineering and Geosciences, University of Newcastle, Newcastle Upon Tyne, UK.

0148-0227/09/2008JF001035

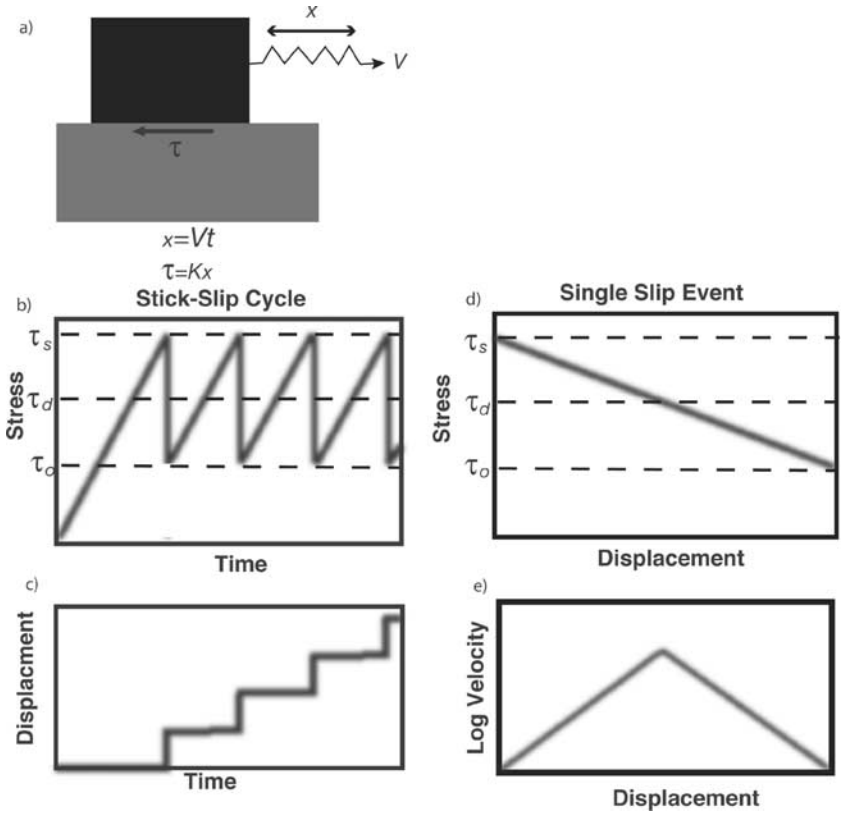

Figure 1. An idealized slider block model of stick-slip motion. (a) A block is loaded under a constant velocity, V, causing extension of the spring, x. Shear stress at the base of the block is calculated using Hooke's law. K is the spring stiffness. (b) This constant loading results in accumulation of stress. (c) When the failure strength of the interface is reached, the block slips, releasing the stored elastic strain. Note this predicts constant recurrence intervals and slip magnitudes. (d) Evolution of stress during a single-slip event. (e) Velocity during a single-slip event. Here τ_s and τ_d are static and dynamic strengths of the block base, and τ_o is the residual stress after slip events end.

collected data set. We then use a simple tidally-modulated ice stream stick-slip model to interpret variability observed in the WIP stick-slip cycle, allowing us to make inferences into the rheology of the subglacial interface.

2. Stick-Slip Motion and the Basal Rheology of Whillans Ice Stream

[5] The movement of WIP is similar to motion on earthquake faults, with long dormant intervals punctuated by short-duration slip events related to the sliding and/or deformation of a thin granular layer (fault gouge or till). As pointed out by *Tulaczyk* [2006], the stick-slip motion observed on WIS serves as a natural slider block experiment, similar to those used in laboratory studies of earthquake and soil mechanics. Thus, understanding the evolution of stress on WIS during stick-slip cycles will enhance our understanding of ice stream physics, and may contribute to the understanding of earthquakes and other related phenomena. Before we discuss the stick-slip motion observed on WIS, we will review the fundamental concepts of stick-slip behavior relevant to our discussion, focusing on the origin of the stick-slip instability. We will then discuss the fundamental implications of stick-slip behavior for our understanding of the basal rheology of ice streams.

2.1. Physics of Stick-Slip Motion

[6] Stick-slip motion in laboratory experiments arises from frictional instabilities associated with the rheology of the sliding interface. Early workers showed that the salient features of stick-slip motion can be reproduced by a plastic rheology (no sliding occurs below a yield strength; see *Byerlee* [1970] for a review). As such, our discussion will focus on the plastic instability for stick-slip motion; however, it is worth noting that this is a crude approximation of the modern understanding of frictional sliding (see *Marone* [1998a] for a review).

[7] The origin of the stick-slip instability can be illustrated by considering the motion of a simple slider block system such as the one shown in Figure 1. The slider block is initially at rest while the attached spring is slowly extended. Extension of the spring results in an increasing force on the block. Friction (shear strength divided by the effective pressure) at the base of the block initially inhibits sliding in response to this force. However, continued extension of a sufficiently strong spring will eventually cause the applied force to be large enough to overcome the frictional resistance at the base of the slider block, causing the block to begin to slide. The observed frictional strength usually changes once sliding begins, from a static to a dynamic value. The change in resistance may be either positive or negative, resulting in two

rheologic end-members that determine whether sliding will be stable or stick slip.

[8] The first possibility is that the system strengthens once sliding begins. A fundamental property of this rheologic end-member is that it is inherently stable; once motion starts, the block will slide smoothly at the rate the spring is being extended. Another fundamental characteristic of this material type is that dynamic friction increases slightly with increasing sliding velocity during steady sliding. For this reason, materials in which dynamic friction exceeds static friction are referred to as velocity-strengthening materials.

[9] Alternatively, resistance to sliding may decrease as sliding begins. In contrast to velocity-strengthening materials, these materials are characterized by an inverse relationship between sliding velocity and dynamic friction, and are referred to as velocity weakening. A consequence of velocity-weakening behavior is the possibility of stick-slip motion. Thus, to understand the sick-slip phenomenon, we will now review the instability associated with velocity-weakening materials.

[10] The origin of the stick-slip instability in velocity-weakening systems can be summarized concisely by schematically examining how the force balance of the system evolves with time and displacement (Figure 1). At the moment sliding begins, resistance to motion drops to the new, lower dynamic value (Figure 1d). At this point the applied force from the spring is higher than that required to maintain motion, resulting in a significant imbalance between the applied force from the spring and resistance at the base of the block. This imbalance results in acceleration of the slider block, producing a peak velocity in the slider block that may be orders of magnitude larger than the velocity of the spring (Figure 1e). The block will continue to accelerate until the spring is compressed to the point that the applied force balances the dynamic frictional strength, at which point the block begins to decelerate. The spring continues to compress as it decelerates, such that the applied force reduces to a value too low to maintain motion, allowing the block to come to rest. After coming to rest, the spring will slowly extend and the process will be repeated (Figures 1b and 1c). An important feature of the stick-slip instability is that slip ends because of a frictional instability, not when the applied force is reduced to zero, resulting in a nonzero residual force from the spring acting on the block.

[11] A fundamental aspect of the slider block system described above is that the style of motion, stable or stick slip, is not dependent on the absolute strength of the sliding interface, but on the difference between static and dynamic strength of the system. Thus, the peak velocities achieved during the slip phase of a stick-slip cycle are not directly related to the applied force at the time slip initiates (as implied by *Tulaczyk* [2006]) but rather to the force imbalance that exists at the onset of slip. The calculations of *Bindschadler et al.* [2003a] indicate that the stress drop averaged over the ice plain during a typical stick-slip event is 0.3 kPa, providing an upper limit on the imbalance between the static and dynamic friction that drives the rapid accelerations observed.

2.2. Stick-Slip Motion of Whillans Ice Stream: Insight Into Rheology

[12] To better predict ice stream dynamics, a set of constitutive equations relating applied basal shear stress and velocity is required. The extreme variations in speed associated with stick-slip motion confirm the highly nonlinear nature of the ice stream bed, and as such it is useful to consider the implications of stick-slip motion for our understanding of subglacial rheology. On the basis of the observation that the beds of many ice streams are often underlain by a water-saturated till, much work has gone into understanding the rheologic behavior of till. Much of this work has focused on determining till rheology from small-scale laboratory experiments. In particular, several studies have been conducted on till retrieved from beneath WIS [*Kamb*, 1991; *Tulaczyk et al.*, 2000b]. However, there has been some debate about extrapolating the small-scale laboratory studies of till, $O(10^{-1}–1$ m), to field scale, $O(1–10^{5}$ m) [e.g., *Fowler*, 2002; *Tulaczyk et al.*, 2000b]. The observation of stick-slip motion makes some fundamental insights into the basal rheology of WIS and the applicability of upscaling the laboratory studies of till.

[13] In laboratory studies, the rheology of a material (velocity strengthening or weakening) is usually determined by measuring the dynamic strength at various sliding speeds. Studies have shown that the rheology of a particular till depends on its physical properties (i.e., grain size, mineralogy, etc.); thus, till may display either velocity weakening or strengthening behavior [e.g., *Iverson et al.*, 1998; *Thomason and Iverson*, 2008]. Tills retrieved from beneath WIS display a slight positive velocity dependence in the laboratory, indicating a velocity-strengthening rheology. However, as we have already noted, a necessary condition for stick-slip sliding is that the rheology of the substrate be velocity weakening; thus, a fundamental inference one can make from observations of stick-slip motion is that the macroscale basal rheology of WIS is most likely velocity weakening. Thus, the small-scale studies of WIS till are not completely consistent with the field observation of stick-slip behavior on WIS as has been recently proposed [*Tulaczyk*, 2006]. While the stick-slip motion confirms the nearly plastic nature of the bed, it also indicates that the bed is likely governed by velocity-weakening physics. The discrepancy between the macroscale behavior of WIS and laboratory-derived till rheology is not surprising, as frictional parameters of materials are often scale dependent [*Marone*, 1998a]. As first noted by *Kamb* [1991, p. 16,587], velocity-weakening behavior of the ice stream bed represents the most extreme version of plastic behavior because of the fact that friction decreases at higher sliding velocities, thus implying a flow law with a negative exponent.

3. Data and Methods

[14] Since the initial observations of tidally-modulated ice stream motion on the Siple Coast of Antarctica, an extensive field program has been carried out to provide the increased spatial and temporal resolution needed to investigate this phenomenon. We exploit a subset of this new data set, acquired during the 2003–2004 and 2004–2005 field seasons on WIS, Mercer Ice Stream (MIS) (formerly known as Ice Stream A) and surrounding regions. Dual-frequency global positioning system (GPS) stations mounted on poles 1.5 meters above the surface and recording at 0.1 Hz were powered by a combination of batteries and solar panels

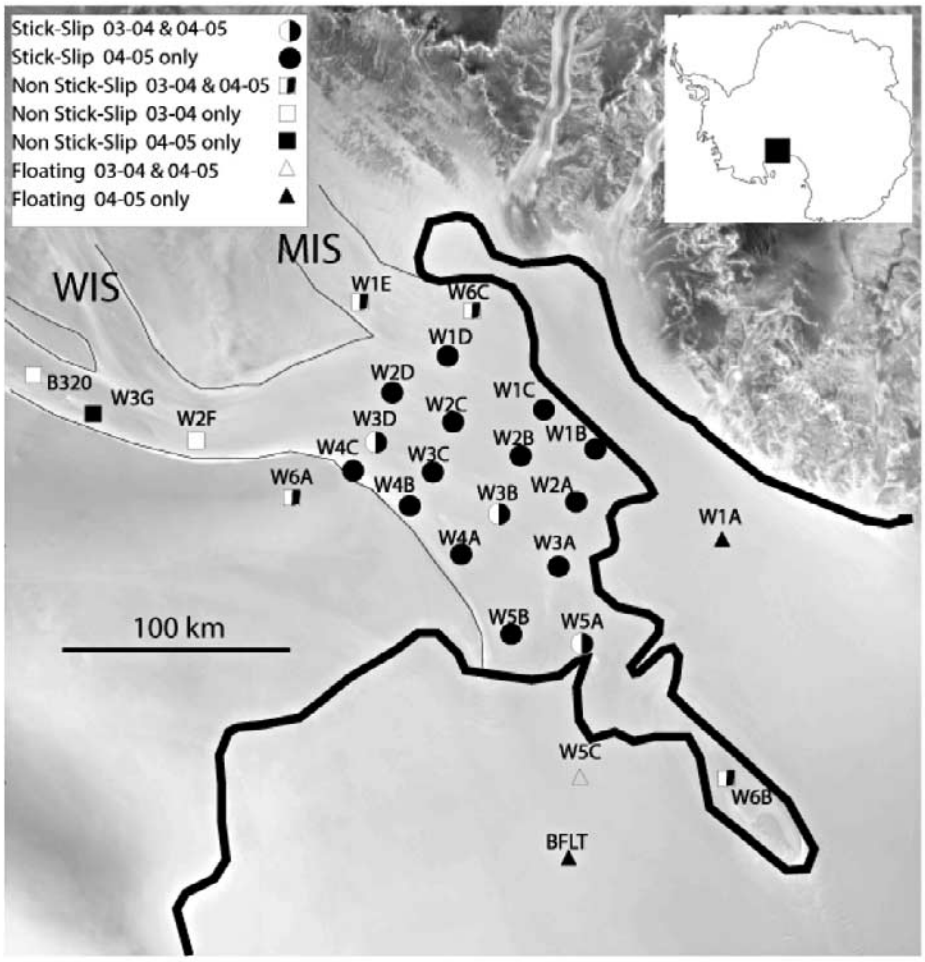

Figure 2. The location examined in this study. Whillans Ice Stream (WIS) and Mercer Ice Stream (MIS) flow from the upper left toward the lower right. Each marker was the location of a GPS occupation, with details of motion and years of occupation indicated by symbol. Thick black line is the grounding line. Thin black line is the margin of WIS and MIS. The style of motion at each site did not change between seasons. Background image is the RADARSAT mosaic (http://nsidc.org/data/ramp/).

during each field season. For 70 days during the first season, five GPS stations were placed on the WIS along a flow line extending from just downstream of the grounding line to 320 km upstream of the grounding line. A more spatially comprehensive array of 20 GPS receivers was deployed for 40 days during the second season. During each season, ice stream stations were supplemented by deployments on neighboring slow-moving ice ridges to aid GPS processing, and just downstream of the grounding line on the ice shelf to measure the ocean tides. Locations and details of station occupation are displayed in Figure 2.

[15] Solutions for receiver position were calculated every 5 minutes using the Precise Point Positioning (PPP) technique in the GIPSY/OASIS software v4 [*Zumberge et al.*, 1997]. A kinematic GPS processing methodology, such as used here, is required in order to minimize GPS-related jumps and periodic signals [*King*, 2004]. This method has been used successfully in previous studies of subdaily variations in ice stream motion [*Anandakrishnan et al.*, 2003; *Bindschadler et al.*, 2003a, 2003b]. Positions are produced with precision of 10 and 30 mm in each of the horizontal and vertical coordinate components, respectively, on the basis of the weighted root-mean-square of the coordinates of a uniformly moving site. For a more detailed discussion of the GPS processing the reader is referred to *King and Aoki* [2003].

4. Tidally-Driven Variability in Stick-Slip Motion

4.1. Stick-Slip Variability

[16] The characteristics of stick-slip motion are shown in Figure 3. Characteristic displacement records representing the two disparate modes of motion found in the WIS/MIS system (stable and stick slip) are shown in Figure 3a. On the basis of the displacement records, we classified each site as smooth or stick slip, to map the spatial extent of stick-slip motion. This analysis confirms the previous observation that the smooth flow is confined to the upstream areas of WIS and MIS (squares in Figure 2), while the entire WIP is dominated by stick-slip motion (circles, Figure 2). Stick-slip motion is similar to that previously observed [*Bindschadler et al.*, 2003a]; long sticky periods are punctuated by short-duration slip events. In total, we observed over 200 distinct slip events

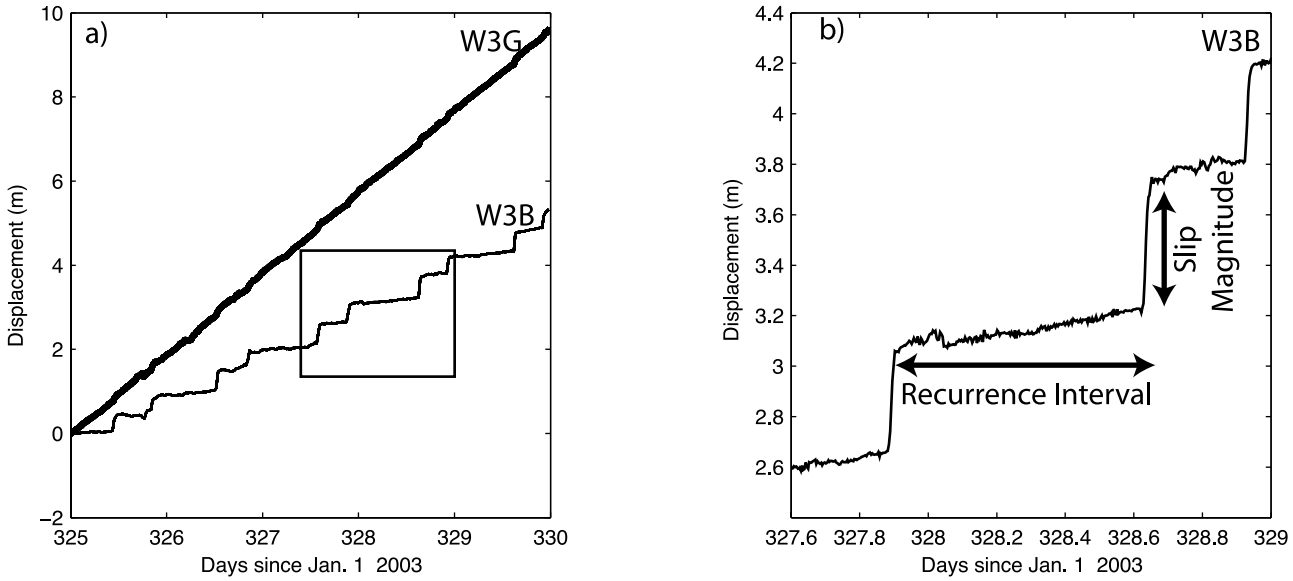

Figure 3. (a) A representative record showing stick-slip motion (W3B, bottom) and a representative record showing smooth motion (W3A, top), spanning the motion styles seen in the study region. The differing average slopes for each station are due to different annual average velocities, 710 m/a for W3G and 370 m/a for W3B. (b) Close up of the box in Figure 3a with recurrence interval (the time between slip events) and slip magnitude (the amount of motion during a slip event) defined.

during the combined 2003–2004 and 2004–2005 field seasons. Two slip events per day were observed on all but 3 of the 110 days of observation; on these 3 occasions just a single slip event was observed.

[17] *Bindschadler et al.* [2003a] first recognized that the time between slip events on WIS varies, and that the timing appears to be correlated with the daily tidal cycle of the Ross Sea (Figure 4). During the spring tide (e.g., day 330, Figure 4), one slip event usually occurs just after high tide, while the subsequent slip event usually occurs just before low tide during the neap tide (e.g., day 324, Figure 4) slip events shift to more uniform spacing in time (12 hours), and are observed on both rising and falling tides. Our new, more extensive data set provides additional insights on many aspects of stick-slip behavior. Here we focus on the relationship between timing and magnitude of slip events as observed at a central location (W3B) that was occupied during both years of our field campaign.

[18] The stick phase of a stick-slip cycle is characterized by minimal motion, as stress accumulates until initiation of the slip event. Thus, it is appropriate to characterize this phase of the cycle by the length of dormancy preceding the slip event. Following terminology used in the earthquake mechanics literature, we refer to this as recurrence interval (Figure 3b). Measurement of recurrence interval for each WIS stick-slip cycle during the 2003–2004 and 2004–2005 field seasons clearly illustrates the correlation of WIS motion with the Ross Sea tides (Figure 5). As previously noted, during the spring tide there is a strong association with the daily tidal cycle, with one slip event just after high tide and one slip event just before low tide (Figure 4). As a result of this tidal phasing, recurrence intervals have a bimodal distribution during spring tides (Figure 5). In contrast, during neap tides when the tidal phasing becomes negligible, recurrence interval becomes more unimodal (Figure 5).

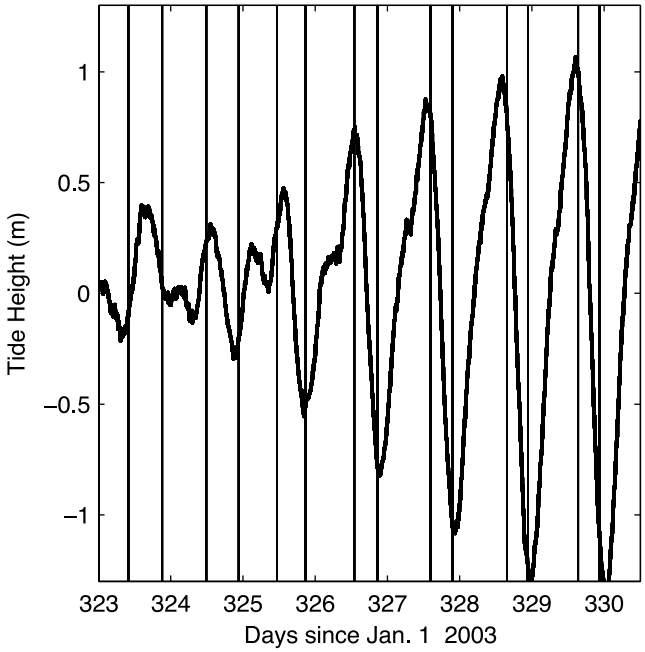

Figure 4. Tidal correlation of slip event timing. Thick line is tidal height of the Ross Sea observed at station BFLT; thin vertical lines are times of slip events. Note that during spring tides (e.g., days 328–331), one event occurs slightly after high tide and one occurs approximately 6 h later slightly before the daily low tide. In contrast, during neap tides (e.g., days 323–325), slip events are more uniformly spaced in time and the association with the tides of the Ross Sea is less clear.

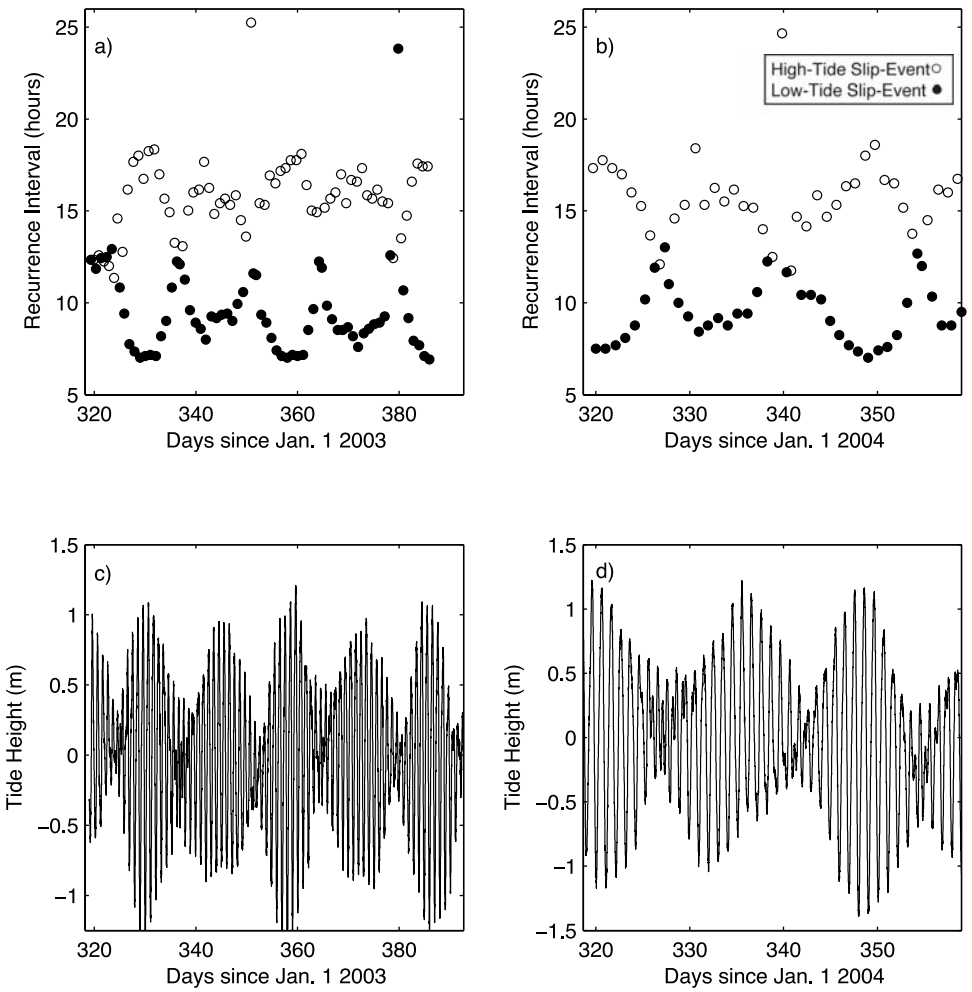

Figure 5. Variability of ice stream stick-slip motion. (a and b) Recurrence interval for the ice plain during each field season. Events are classified as either high tide (open symbols) or low tide (solid symbols) on the basis of whether the event occurred closer in time to a peak high or low tide. (c and d) Tide during each field season, observed at BFLT during 2003–2004 and W5C for 2004–2005. The results highlight the tidal correlation between the stick-slip cycle and the Ross Sea tides. During neap tides, slip events are more uniformly spaced in time (convergence of open and solid symbols) in contrast to the tidal modulated timing of slip events during spring tides (divergence of open and solid symbols).

[19] In contrast to the "stick" phase of the stick-slip cycle, the slip phase is relatively short in duration, but experiences a large amount of displacement. For this reason, the slip phase of the stick-slip cycle can be characterized by measuring the total displacement that occurs during the slip event, which we call slip magnitude (Figure 3b). While previous work highlighted the variable timing of slip events, our measurements reveal that the amount of slip that occurs during a slip event is also modulated. The most prominent feature of slip magnitude variation is a positive correlation with the length of the recurrence interval that precedes the slip event (Figure 6).

4.2. Tidally-Driven Stick-Slip Model

[20] The stick-slip instability is due to the imbalance in forces that exist at the beginning of a slip event. We perform a simple analysis to calculate the forces acting on the stick-slip section of WIS, and estimate the magnitude of the imbalances associated with ice stream stick-slip motion. Given the repeatability of the WIS stick-slip events, we assume that the accumulated stress during the stick phase must equal the stress released during the slip event. This must be true over long timescales (weeks to years) though we cannot rule out variations over shorter timescales (days). We begin with the simplest assumption. To understand the stick-slip cycle requires understanding how stress evolves prior to the slip event. We calculate the mean accumulated basal stresses during the stick part of the cycle using a simple slider block representation of the ice plain [*Bindschadler et al.*, 2003a].

[21] We assume that an ice stream such as WIS that terminates in the ocean or an ice shelf has its stress modified by forcings at the upstream and downstream ends of the sticky region (Figure 7). Upstream of the stick-slip region, the ice stream flows at a constant velocity (Figure 3), inducing a linear increase in elastic strain in the stagnant lower reaches of the ice stream, similar to the loading of the spring in Figure 1. At the grounding line, tidal fluctuations in sea

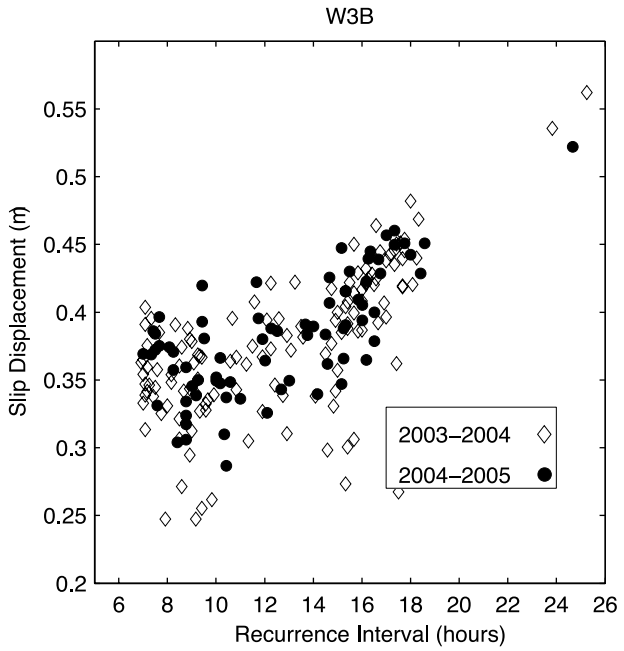

Figure 6. Slip magnitude as a function of recurrence interval for station W3B. The data show that a positive correlation exists between the length of dormancy preceding a slip event and the total displacement during a slip event.

surface height influence flow by introducing changes in the force resisting forward motion of the glacier. For the Siple Coast, this phenomenon was observed first in records of basal seismicity on Kamb Ice Stream (formerly Ice Stream C) [*Anandakrishnan and Alley*, 1997] and more recently from GPS-derived surface velocities on Bindschadler Ice Stream (formerly Ice Stream D) [*Anandakrishnan et al.*, 2003]. The resistance of the ocean to ice stream motion is related to the height of the water column. The nonfloating portion of the ice stream experiences higher pressure from the water at high tide than at low tide; thus, the tides impart an approximately sinusoidal fluctuation to the stress regime.

[22] The WIP can be modeled as a slider block of length L = 150 km, and height H = 750 m. We assume that during the "stick" phase the imbalance of forces on this block is balanced by the basal friction. In our simple model we ignore the contribution of side drag as it is expected to be small because of the width of the WIP. *Bindschadler et al.* [2003a] showed that the time evolution of the average basal shear stress of the WIP can be represented as

$$\overline{\tau}_b(t) = \overline{\tau}_o + \frac{Vt_0EH}{L^2} - \frac{\rho_i g h(t) H}{L}, \qquad (1)$$

where τ_o is a residual basal shear stress at the end of a slip event, E is the elastic modulus of ice, g is gravitational acceleration, $h(t)$ is the tidal height measured in the Ross Sea, V is the velocity upstream of the sticking region, t_0 is the time since the last slip event, and ρ_i is the density of ice. The second term on the right side accounts for the upstream loading ($\overline{\tau}_{\text{upstream}}$ in Figure 7), while the third term accounts for the tidal fluctuations ($\overline{\tau}_{\text{tide}}$ in Figure 7). We use equation 1 to calculate the evolution of basal stress for each observed slip event. However, since we have limited knowledge of $\overline{\tau}_o$, our results will focus on the accumulated basal shear stress during each stick-slip cycle, $\overline{\tau}_b(t) - \overline{\tau}_o$.

4.3. Model Results

[23] We begin discussion of the model results by examining three stick-slip cycles that cover the range of observed recurrence intervals: short, medium, and long (Figure 8). Each time series covers an entire stick-slip cycle, beginning just after the termination of a slip event and concluding at the termination of the subsequent slip event (Figures 8a–8c). Figures 8a–8c show the displacement for station W3B during each stick-slip cycle, displaying the characteristic increase in slip magnitude at longer recurrence intervals. Figures 8d–8f show the Ross Sea tides as determined by the vertical component of a station located on the Ross Ice Shelf (BFLT for 2003–2004 and W5C for 2004–2005). As discussed earlier, each style of stick-slip cycle is associated with a particular state of the Ross Sea tides. Short and long recurrence interval stick-slip cycles occur during spring tides with median length stick-slip cycles during neap tides. The modeled stress evolution during each stick-slip cycle is shown in Figures 8g–8i. During the stick phase of the stick-slip cycle, basal shear stress slowly accrues until slip of the ice plain initiates and displacement relieves stress, returning stress on the system to a background level, $\overline{\tau}_o$.

[24] A primary motivation of our modeling is to investigate the observed correlation between the tides of the Ross Sea and the stick-slip motion of WIS. For this reason, in addition to the total stress curve (solid line) we have plotted the upstream (dashed line) and tidal component (dotted line) individually (Figures 8g–8i) to elucidate the individual contributions from each component. It is clear for each example that the majority of modeled accumulated stress during a stick-slip cycle results from the upstream component, while sinusoidal tidal forcing results in small modifications to the stress evolution. Although they are small, tidally-driven stress fluctuations introduce variations in the rate at which stress is applied to the system, which depends on the tidal phase during the stick-slip cycle [*Bindschadler et al.*, 2003a]. For a stick-slip cycle occurring on a rapidly falling tide, such as typical short stick-slip cycles (Figures 8a, 8d, and 8g), the effect is to increase the loading rate at which stress is accumulated compared to the upstream loading alone. The

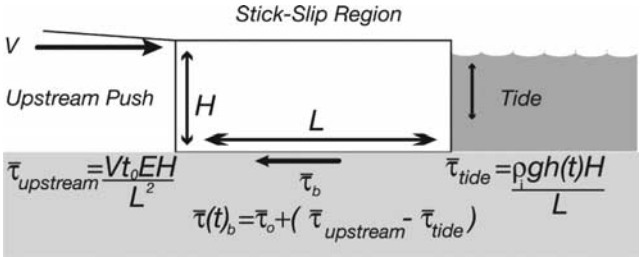

Figure 7. Our model of ice stream stick slip (equation (1)); see text for explanation of variables. The block experiences forces induced by the continuing motion of the ice upstream of the block, $\overline{\tau}_{\text{upstream}}$, and from tidal variations $\overline{\tau}_{\text{tide}}$ [*Bindschadler et al.*, 2003a].

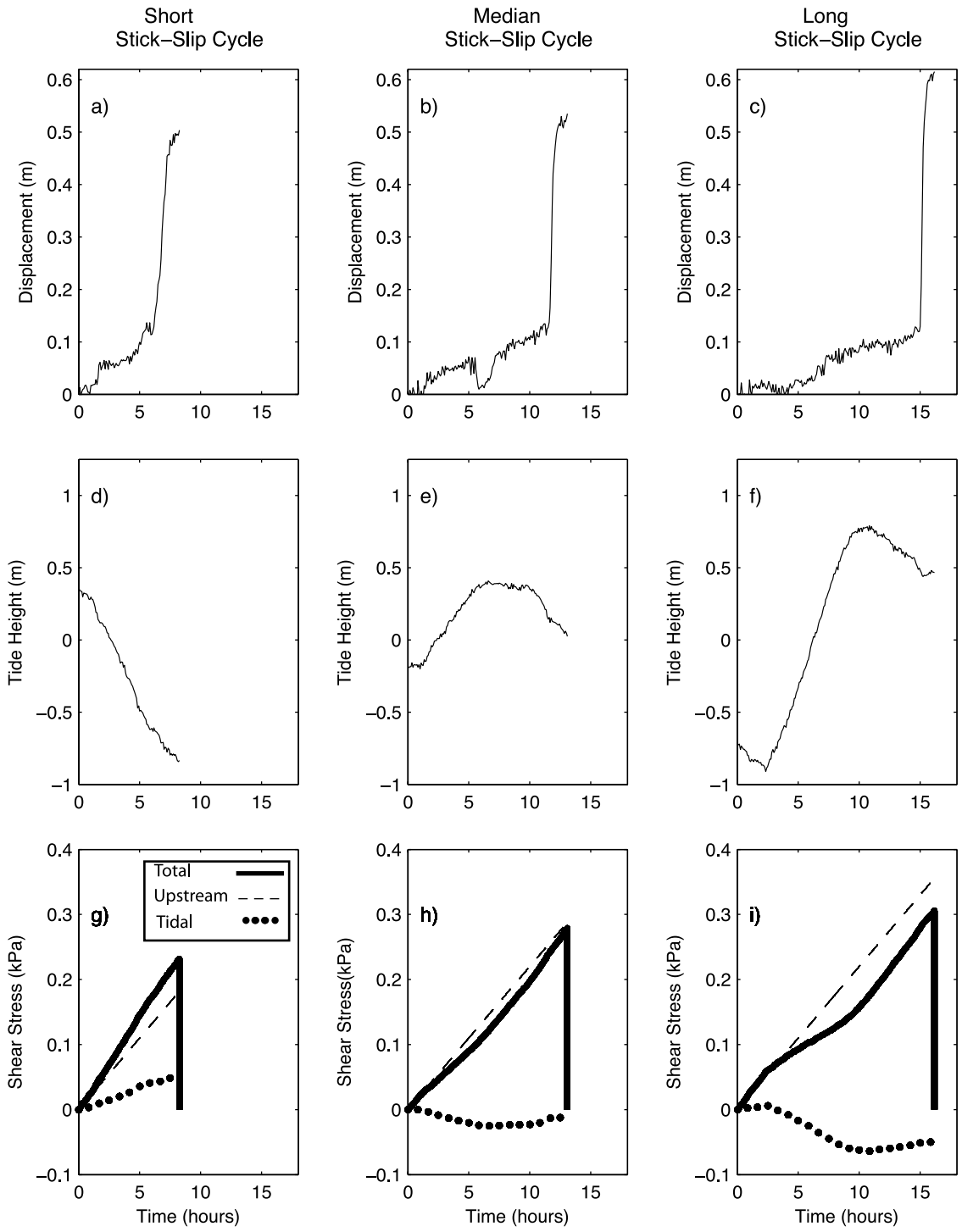

Figure 8. Examples of stress evolution during ice stream stick-slip cycles. (a–c) Displacement during the stick-slip cycles. (d–f) Tidal fluctuations in the Ross Sea during the stick-slip cycles. (g–i) Shear stress evolution, $\overline{\tau}_b - \overline{\tau}_o$, during the stick-slip cycles. Solid line is the total modeled shear stress, dashed line is the upstream component, and dotted line is the tidal component.

opposite effect is seen for stick-slip cycles that occur during predominantly rising tides, as is the case for stick-slip cycles with long recurrence intervals (Figures 8c, 8f, and 8i). Medium recurrence interval stick-slip cycles occur during the neap tide, and the linear upstream loading dominates the accumulation of shear stress (Figures 8b, 8d, and 8h) [*Bindschadler et al.*, 2003a].

[25] The tidal effect on stress accumulation can be quantified by measuring an average loading rate for each stick-slip cycle ($\frac{\Delta\overline{\tau}}{\Delta t}$), the slope of the total stress evolution curve.

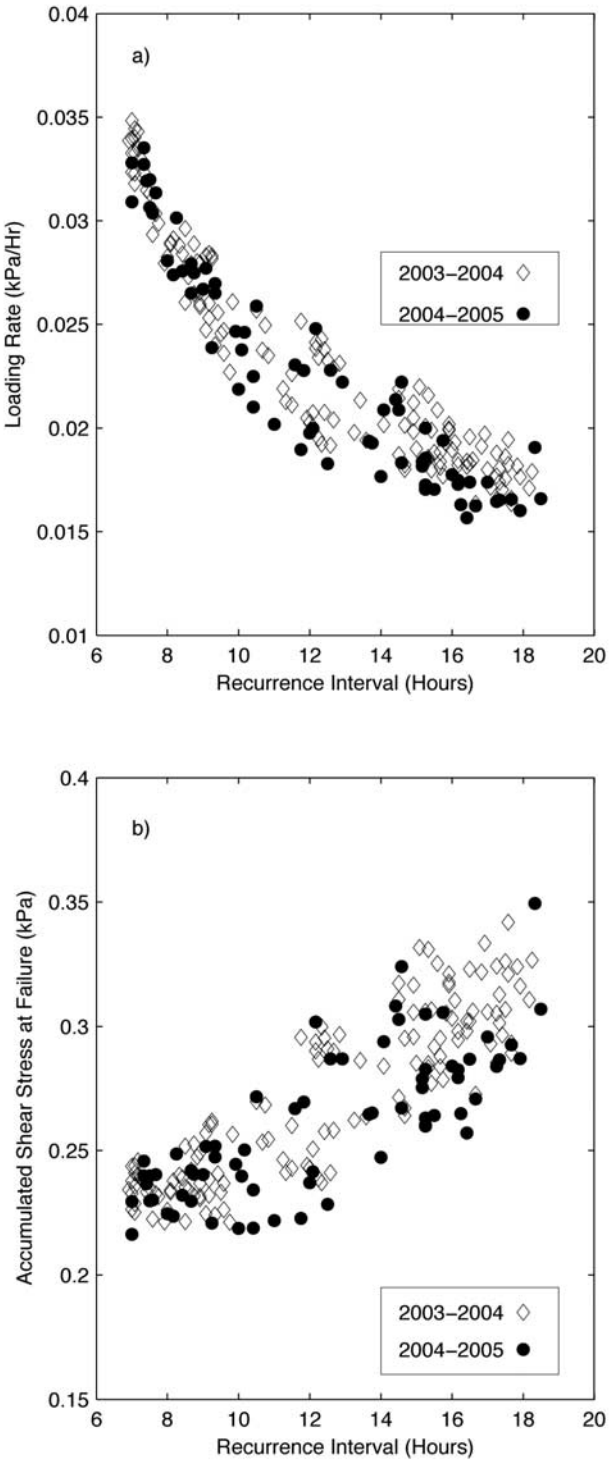

Figure 9. Summary of modeling results. The (a) loading rate and (b) total accumulated stress during the stick phase of each stick-slip cycle. Both loading rate and accumulated shear stress are related to recurrence interval.

We have done this for each of our observed slip events (Figure 9a), showing the clear inverse relationship between average loading rate and recurrence interval. The modeled accumulated shear stress at slip initiation shows an increasing at trend at longer recurrence intervals (Figures 8g–8i). Thus, we have also measured the modeled accumulated shear stress that precedes each slip event (Figure 9b).

5. Discussion

[26] Our data show significant variability in the WIS stick-slip cycle, and our model provides a context for understanding this variability. The WIS usually experiences two slip events per day; however, the temporal separation of consecutive events varies. In particular, the contrasting behavior of bimodal timing of stick-slip cycles during spring tides versus the more unimodal spacing of stick-slip events during neap tides requires an explanation. Figure 9a shows inverse dependence of recurrence interval on loading rate across a broad range of loading rates.

[27] A similar relationship between loading rate and recurrence interval is seen in both numerical and laboratory studies of stick-slip behavior [e.g., *Karner and Marone*, 2000]. One reason for this behavior, along with an increase in bed strength over time, as discussed below, is that an increase in loading rate reduces the time needed to reach the yield stress of the sliding interface; conversely, a reduction in loading rate increases the time to reach a given yield stress. As discussed in the previous section, ocean tides drive loading rate variations (Figure 9a). For this reason, under the less variable loading that occurs during neap tides, stick-slip cycles are relatively uniform in duration as the tides only marginally affect the rate at which stress is applied to the stick-slip section of the ice stream. In contrast, spring tides introduce relatively high loading rates on the falling tides and relatively low loading rates on the rising tides, introducing the correlation observed between the timing of slip events and the daily tidal cycle as seen in Figure 4 [*Bindschadler et al.*, 2003a].

[28] The tidal forcing of loading rate provides an explanation for the timing of slip events; however, this cannot account for the observed variations in slip magnitude. Observed displacements during slip events that occur after long recurrence intervals can be up to twice as large as displacements that occur after short recurrence intervals. In stick-slip regimes, the displacement that occurs during slip events provides a mechanism for the release of the stored elastic strain acquired during the stick phase of the stick-slip cycle. For this reason, the magnitude of a slip event will be directly related to the amount of accumulated shear stress that accrues during the stick phase. The modeled accumulated shear stress provides insight into the origin of this pattern. Figure 9b shows larger accumulated shear stress at time of slip initiation for those events that occur after longer recurrence intervals. Thus, the increase in slip magnitude that occurs at increased recurrence intervals is due to an increase in accumulated shear stress.

[29] An important implication of these results is that the yield strength of the ice stream bed increases with time following termination of a slip event. Fortuitously, previous theoretical and empirical studies of stick-slip motion provide a physical framework to understand the variability in the yield strength of subglacial bed. A significant body of research has shown that the yield strength of an interface will increase following the end of a slip event [e.g., *Dieterrich*, 1972; *Marone*, 1998b]. This phenomenon, associated with the sliding of solid surfaces past one another as well as

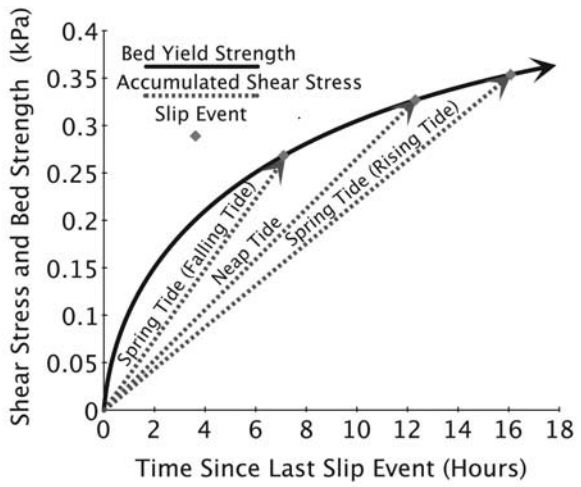

Figure 10. Subglacial healing and observed stick-slip cycles on WIS. At the beginning of each stick-slip cycle, shear stress is reduced to $\overline{\tau}_o$, and subsequently stress increases. At the same time, the yield strength of the bed slowly increases. A slip event initiates when the bed strength curve and accumulated stress curve intersect. During neap tides, slip events are of more uniform spacing and during spring tides end-members for both recurrence interval and slip magnitude occur.

during the shear of granular materials, is known as healing. Healing is a complex phenomenon (see *Marone* [1998a] for a review), which may be associated with several different processes such as the interaction of asperities at a sliding interface or grain rearrangement of a shearing layer. Thus, while variability in bed strength of ice streams is usually considered to have characteristic timescales of order of years, largely dependent on the mass balance of water near the bed of the ice stream [e.g, *Tulaczyk et al.*, 2000b], our results show that the bed of an ice stream is capable of relatively large variations, >0.35 kPa, relative to the strength of the bed, likely <5 kPa [*Joughin et al.*, 2004a], during the course of a single day.

[30] Time-dependent strength at the bed of WIS is likely regulated by the tendency of the ice stream to freeze onto its bed [e.g., *Joughin et al.*, 2004b]. Weakening of the bed during slip events may be accomplished through the combination of sediment dilation, frictional heating, and disruption of the water system. If motion is dominated by till deformation, freezing during the stick phase would tend to dewater and strengthen the till [*Christoffersen and Tulaczyk*, 2003]. Deciphering the exact physics responsible for the observed healing may lead to a much improved understanding of ice stream stick-slip motion; however, it is beyond the scope of this contribution.

[31] The correlation observed between the character of stick-slip motion and the tidal phases of the Ross Sea can now be explained if we incorporate a theory of subglacial healing into the basal mechanics of ice stream stick-slip motion (Figure 10). Following the termination of a slip event, the yield strength of the bed and the accumulated shear stress increase (Figure 10). Initially healing must increase the bed strength at a rate higher than stress is accumulated to prevent initiation of a slip event. Thus, while the shape of the healing curve is constrained only in the time range of 6–18 h when the healing curve must pass through modeled stress data (Figure 9b), an increasing concave down profile is needed to explain the lack of shorter recurrence interval slip events (less than approximately 6 hours). The concave down profile may be explained by several physically reasonable processes. If healing is controlled by freeze-on processes, strengthening should become less efficient as time progresses. For example, if healing is associated with the freezing of the ice stream onto sticky spots, over time heat must be conducted through a thickening layer of accreted basal ice. Likewise, the rate of strengthening driven by the dewatering of till would decrease over time because of reduced permeability of the till [*Tulaczyk et al.*, 2000a]. During neap tides, the upstream forcing dominates and stress is loaded to the system at a relatively uniform rate; thus, the stress evolution curve intersects the strength-time curve more uniformly, producing a stick-slip cycle that more closely resembles the idealized case shown in Figure 1, in which recurrence interval and slip magnitude are repeated with little variation between consecutive events. In contrast, spring tides introduce fluctuations into the stress evolution of the ice stream, resulting in deviations from the mean slip magnitude and recurrence interval. On a more rapidly falling tide, the stress-time curve intersects the strength-time curve earlier in the stick-slip cycle. A consequence of this early failure is that less shear stress has been accumulated, resulting in lower slip magnitudes. In contrast, a stick-slip cycle that occurs over a predominantly rising tide during spring tide experiences a relatively low rate of accumulation of net shear stress, providing the bed of the ice stream additional time to heal; thus, additional shear stress is required to promote failure, and as a consequence larger slip magnitudes are produced.

6. Summary

[32] Stick-slip behavior suggests that the basal rheology of the WIS behaves in a velocity weakening manner, indicating that the rheology of the WIS bed may be more prone to unstable flow than suggested by traditional flow laws [*Kamb*, 1991]. The variability observed in the stick-slip behavior of WIS can be easily understood within the framework of a tidally modulated stress regime. Healing during quiescence (“stick” intervals) strengthens the bed, so that a slower rate of stress accumulation caused by tidal forcing leads to a longer interval between slip events, and to a larger magnitude slip in response to the larger stress imbalance accumulated during the longer interval. Our observations provide additional useful constraints on the understanding of the ice sheet bed and motivate additional work toward better understanding of the basal physics of ice streams.

[33] **Acknowledgments.** This work was funded by the US National Science Foundation (NSF-OPP-0229659). M.A.K. was partly funded by a NERC fellowship. We thank Raytheon Polar Services, the New York Air National Guard, and Ken Borek Air for logistical support; UNAVCO for providing GPS receivers; as well as Don Voigt, Huw Horgan, Ian Joughin, and Leo Peters for help with the field deployment. Comments by Gordon Hamilton, Kelly Brunt, and an anonymous reviewer improved the manuscript.

References

Alley, R. B., D. D. Blankenship, C. R. Bentley, and S. T. Rooney (1987), Till beneath Ice Stream B: 3. Till deformation—Evidence and implications, *J. Geophys. Res.*, *92*(B9), 8921–8929.

Anandakrishnan, S., and R. B. Alley (1997), Tidal forcing of basal seismicity of Ice Stream C, West Antarctica, observed far inland, *J. Geophys. Res.*, *102*(B7), 15,183–15,196.

Anandakrishnan, S., D. E. Voigt, R. B. Alley, and M. A. King (2003), Ice stream D flow speed is strongly modulated by the tide beneath the Ross Ice Shelf, *Geophys. Res. Lett.*, *30*(7), 1361, doi:10.1029/2002GL016329.

Bindschadler, R. (1993), Siple Coast Project research of Crary Ice Rise and the mouths of ice streams B and C, West Antarctica: Review and new perspectives, *J. Glaciol.*, *39*(133), 538–552.

Bindschadler, R. A., M. A. King, R. B. Alley, S. Anandakrishnan, and L. Padman (2003a), Tidally controlled stick-slip discharge of a west Antarctic ice stream, *Science*, *301*(5636), 1087–1089.

Bindschadler, R. A., P. L. Vornberger, M. A. King, and L. Padman (2003b), Tidally driven stick-slip motion in the mouth of Whillans Ice Stream, Antarctica, *Ann. Glaciol.*, *36*, 263–272.

Blankenship, D. D., C. R. Bentley, S. T. Rooney, and R. B. Alley (1986), Seismic measurements reveal a saturated porous layer beneath an active Antarctic ice stream, *Nature*, *322*(6074), 54–57.

Brace, W., and J. Byerlee (1966), Stick-slip as a mechanism for earthquakes, *Science*, *153*, 990–992.

Byerlee, J. (1970), The mechanics of stick-slip, *Tectonophysics*, *9*, 475–486.

Christoffersen, P., and S. Tulaczyk (2003), Response of subglacial sediments to basal freeze-on: 1. Theory and comparison to observations from beneath the West Antarctic Ice Sheet, *J. Geophys. Res.*, *108*(B4), 2222, doi:10.1029/2002JB001935.

Dieterrich, J. (1972), Time-dependent friction in rocks, *J. Geophys. Res.*, *77*, 3690–3697.

Engelhardt, H., and B. Kamb (1998), Basal sliding of Ice Stream B, west Antarctica, *J. Glaciol.*, *44*(147), 223–230.

Engelhardt, H., N. Humphrey, B. Kamb, and M. Fahnestock (1990), Physical conditions at the base of a fast moving Antarctic ice stream, *Science*, *248*(4951), 57–59.

Fowler, A. C. (2002), Rheology of subglacial till, *J. Glaciol.*, *48*(163), 631–632.

Gudmundsson, G. H. (2007), Tides and the flow of Rutford Ice Stream, west Antarctica, *J. Geophys. Res.*, *112*, F04007, doi:10.1029/2006JF000731.

Iverson, N. R., T. S. Hooyer, and R. W. Baker (1998), Ring-shear studies of till deformation: Coulomb-plastic behavior and distributed strain in glacier beds, *J. Glaciol.*, *44*(148), 634–642.

Joughin, I., and S. Tulaczyk (2002), Positive mass balance of the Ross Ice Streams, West Antarctica, *Science*, *295*(5554), 476–480.

Joughin, I., D. R. MacAyeal, and S. Tulaczyk (2004a), Basal shear stress of the Ross Ice Streams from control method inversions, *J. Geophys. Res.*, *109*, B09405, doi:10.1029/2003JB002960.

Joughin, I., S. Tulaczyk, D. R. MacAyeal, and H. Engelhardt (2004b), Melting and freezing beneath the Ross Ice Streams, Antarctica, *J. Glaciol.*, *50*(168), 96–108.

Kamb, B. (1991), Rheological nonlinearity and flow instability in the deforming bed mechanism of ice stream motion, *J. Geophys. Res.*, *96*(B10), 16,585–16,595.

Karner, S., and C. Marone (2000), Effects of loading rate and normal stress on stress drop and stick-slip recurrence interval, in *Geocomplexity and Physics of Earthquakes*, *Geophys. Monogr. Ser.*, vol. 120, edited by J. B. Rundle, D. L. Turcotte, and W. Klein, pp. 187–198, AGU, Washington, D. C.

King, M. (2004), Rigorous GPS data processing strategies for glaciological applications, *J. Glaciol.*, *50*(171), 601–607.

King, M., and S. Aoki (2003), Tidal observations on floating ice using a single GPS receiver, *Geophys. Res. Lett.*, *30*(3), 1138, doi:10.1029/2002GL016182.

Marone, C. (1998a), Laboratory-derived friction laws and their application to seismic faulting, *Annu. Rev. Earth Planet. Sci.*, *26*, 643–696.

Marone, C. (1998b), The effect of loading rate on static friction and the rate of fault healing during the earthquake cycle, *Nature*, *391*, 69–72.

Murray, T., A. M. Smith, M. A. King, and G. P. Weedon (2007), Ice flow modulated by tides at up to annual periods at Rutford Ice Stream, west Antarctica, *Geophys. Res. Lett.*, *34*, L18503, doi:10.1029/2007GL031207.

Rathbun, A., C. Marone, R. B. Alley, and S. Anandakrishnan (2008), Laboratory study of the fricitonal rheology of sheared till, *J. Geophys. Res.*, *113*, F02020, doi:10.1029/2007JF000815.

Rooney, S. T., D. D. Blankenship, R. B. Alley, and C. R. Bentley (1987), Till beneath Ice Stream B: 2. Structure and continuity, *J. Geophys. Res.*, *92*(B9), 8913–8920.

Thomason, J., and N. R. Iverson (2008), A laboratory study of particle ploughing and pore-pressure feedback: A velocity-weakening mechanism for soft glacier beds, *J. Glaciol.*, *54*(184), 169–181.

Tulaczyk, S. (2006), Scale independance of till rheology, *J. Glaciol.*, *178*, 377–380.

Tulaczyk, S., W. B. Kamb, and H. F. Engelhardt (2000a), Basal mechanics of Ice Stream B, West Antarctica: 2. Undrained plastic bed model, *J. Geophys. Res.*, *105*(B1), 483–494.

Tulaczyk, S., W. B. Kamb, and H. F. Engelhardt (2000b), Basal mechanics of Ice Stream B, West Antarctica: 1. Till mechanics, *J. Geophys. Res.*, *105*(B1), 463–481.

Zumberge, J., M. Heflin, D. Jefferson, M. Watkins, and F. Webb (1997), Precise point positioning for the efficient and robust analysis of GPS data from large networks, *J. Geophys. Res.*, *102*(B3), 5005–5017.

R. B. Alley and S. Anandakrishnan, Center for Remote Sensing of Ice Sheets, Department of Geosciences, Penn State University, 538 Deike Building, University Park, PA 16802, USA.

R. A. Bindschadler, Hydrospheric and Biospheric Sciences Laboratory, NASA Goddard Space Flight Center, Mail Code 614, 8800 Greenbelt Road, Greenbelt, MD 20770, USA.

M. A. King, School of Civil Engineering and Geosciences, University of Newcastle, Cassie Building, Newcastle Upon Tyne NE1 7RU, UK.

J. P. Winberry, Department Geological Sciences, Central Washington University, 400 East University Way, Ellensburg, WA 98926, USA. (winberry@geology.cwu.edu)